NASA/TM—2003-212225 AIAA–2003–0672

Decomposing Solid Micropropulsion Nozzle Performance Issues

Brian Reed
Glenn Research Center, Cleveland, Ohio

May 2003

The NASA STI Program Office . . . in Profile

Since its founding, NASA has been dedicated to the advancement of aeronautics and space science. The NASA Scientific and Technical Information (STI) Program Office plays a key part in helping NASA maintain this important role.

The NASA STI Program Office is operated by Langley Research Center, the Lead Center for NASA's scientific and technical information. The NASA STI Program Office provides access to the NASA STI Database, the largest collection of aeronautical and space science STI in the world. The Program Office is also NASA's institutional mechanism for disseminating the results of its research and development activities. These results are published by NASA in the NASA STI Report Series, which includes the following report types:

- TECHNICAL PUBLICATION. Reports of completed research or a major significant phase of research that present the results of NASA programs and include extensive data or theoretical analysis. Includes compilations of significant scientific and technical data and information deemed to be of continuing reference value. NASA's counterpart of peer-reviewed formal professional papers but has less stringent limitations on manuscript length and extent of graphic presentations.

- TECHNICAL MEMORANDUM. Scientific and technical findings that are preliminary or of specialized interest, e.g., quick release reports, working papers, and bibliographies that contain minimal annotation. Does not contain extensive analysis.

- CONTRACTOR REPORT. Scientific and technical findings by NASA-sponsored contractors and grantees.

- CONFERENCE PUBLICATION. Collected papers from scientific and technical conferences, symposia, seminars, or other meetings sponsored or cosponsored by NASA.

- SPECIAL PUBLICATION. Scientific, technical, or historical information from NASA programs, projects, and missions, often concerned with subjects having substantial public interest.

- TECHNICAL TRANSLATION. English-language translations of foreign scientific and technical material pertinent to NASA's mission.

Specialized services that complement the STI Program Office's diverse offerings include creating custom thesauri, building customized databases, organizing and publishing research results . . . even providing videos.

For more information about the NASA STI Program Office, see the following:

- Access the NASA STI Program Home Page at ***http://www.sti.nasa.gov***

- E-mail your question via the Internet to help@sti.nasa.gov

- Fax your question to the NASA Access Help Desk at 301–621–0134

- Telephone the NASA Access Help Desk at 301–621–0390

- Write to:
  NASA Access Help Desk
  NASA Center for AeroSpace Information
  7121 Standard Drive
  Hanover, MD 21076

NASA/TM—2003-212225 AIAA–2003–0672

Decomposing Solid Micropropulsion Nozzle Performance Issues

Brian Reed
Glenn Research Center, Cleveland, Ohio

Prepared for the
41st Aerospace Sciences Meeting and Exhibit
sponsored by the American Institute of Aeronautics and Astronautics
Reno, Nevada, January 6–9, 2003

National Aeronautics and
Space Administration

Glenn Research Center

May 2003

Available from

NASA Center for Aerospace Information
7121 Standard Drive
Hanover, MD 21076

National Technical Information Service
5285 Port Royal Road
Springfield, VA 22100

Available electronically at http://gltrs.grc.nasa.gov

Decomposing Solid Micropropulsion Nozzle Performance Issues

Brian Reed
National Aeronautics and Space Administration
Glenn Research Center
Cleveland, Ohio 44135

Abstract

Micropropulsion technology is essential to the success of miniaturized spacecraft and can provide ultra-precise propulsion for small spacecraft. NASA Glenn Research Center has envisoned a micropropulsion concept that utilizes decomposing solid propellants for a valveless, leak-free propulsion system. Among the technical challenges of this decomposing solid micropropulsion concept is optimization of miniature, rectangular nozzles. A number of flat micronozzles were tested with ambient-temperature nitrogen and helium gas in a vacuum facility. The thrusters were etched out of silicon and had throat widths on the order of 350 microns and throat depths on the order of 250 microns. While these were half-sections of thrusters (two would be bonded together before firing), testing provided the performance trend for nozzles of this scale and geometry. Area ratios from 1 to 25 were tested, with thrust measured using an inverted pendulum thrust stand for nitrogen flows and a torsional thrust stand for helium. In the nitrogen testing, peak nozzle performance was achieved around area ratio of 5. In the helium testing, nozzle performance peaked for the smallest nozzle tested, area ratio 1.5. For both gases, there was a secondary performance peak above area ratio 15. At low chamber pressures (< 1.6 atm), nitrogen provided higher nozzle performance than helium. The performance curve for helium was steeper, however, and it appeared that helium would provide better performance than nitrogen at higher chamber pressures.

Introduction

In recent years, there has been interest (primarily in government and academia sectors) toward shrinking the size of spacecraft, so that the costs and risk of missions can be reduced.[1,2] Spacecraft in the range of 20- to 100-kg represent the class most likely to be utilized by most "small satellite" users in the near future. There are efforts to develop 10- to 20-kg class spacecraft for use in satellite constellations. There are more ambitious efforts to develop spacecraft less than 10-kg, employing micro-electricalmechanical systems (MEMS) fabrication technology. Obviously, as spacecraft size decreases the difficulty in miniaturizing spacecraft systems increases (size is given here in terms of mass, but the implications for the volume envelope are even more severe).

Propulsion represents the most challenging spacecraft system to miniaturize. There is a point where reduced-scale versions of conventional propulsion systems will no longer be practical. This restriction is not only a result of practical volume, mass, and power limitations, but also of the physics at reduced scale, where forces ignored at conventional scale become dominant.[3] At this point, a fundamentally different approach to propulsion must be taken. To address this need various efforts are underway to develop unique miropropulsion technologies for miniature spacecraft applications.[4,5,6] Micropropulsion systems not only have to be reduced scale in mass and volume, but also use little or no power, be relatively simple yet flexible enough to use in multiple functions, and be cost effective for what is likely to be a relatively low-cost spacecraft.

Micropropulsion applications would not be necessary restricted to MEMS spacecraft as micropropulsion can be used to conduct precision maneuvers for larger spacecraft. Functions for larger spacecraft include spin-up and spin-down, precision positioning and pointing, constellation maintenance, and deorbiting. Grouping micropropulsion systems in arrays will allow their use for larger thrust applications. These "macroscale" functions of micropropulsion may ultimately be the first application of this technology.

This report concerns a valveless, flexible micropropulsion system that uses decomposing solids as propellants.[7] The concept would use an array composed of hundreds (or thousands, as necessary) of MEMS thruster units, arranged in the

configuration best suited for a particular application. Different thruster sizes (throat areas, nozzle area ratios) would provide for a range of thrust levels (from μN's to mN's) within the same array. Several thrusters could be fired simultaneously for thrust levels higher than the basic units, or in a rapid sequence in order to provide gradual but steady low-g acceleration. Decomposing solid propellant pellets (slow-burning propellants referred to as gas generators) would provide long-term, leak-free storage. Initiation of the propellants would be accomplished with a diode laser-based, fiber-optic network. Silicon is transparent at wavelengths above 1.3 microns, allowing laser penetration and initiation without structure-compromising feedthroughs. Power requirements for initiation would be less than 100 milliwatts.

For this decomposing solid micropropulsion concept, there are five major technology challenges that need to be addressed, summarized in Table I. Reliable, reproducible fabrication of miniature thrusters having widths on the order of 300 microns and aspect ratios of at least 2:1 is a critical aspect of many micropropulsion efforts. Since, in this concept, thrusters are likely to be composed of two half-sections to allow the propellant grain to be inserted in the chamber, bonding of half-sections without initiating the propellant is a critical procedure in thruster fabrication. Another technical challenge is selection of the decomposing solid propellant. The propellant needs to provide high performance (Isp > 200 sec) in a low-heat flux decomposition process with benign decomposition products. The initiation of propellant using a diode laser represents a technical challenge that is key to this micropropulsion concept. Initiation of propellant through the thruster walls provides for a valveless, leak-free system, but care must be taken not to create a burdensome system of fiber optics and power requirements need to be low. Finally, the individual components (microthrusters with propellant, initiation system) must be packaged into an array that can be configured for multiple and different spacecraft propulsion functions.

The issue of optimization of rectangular nozzles, subjected to low Reynolds number, viscous-dominated flows is the subject of this report. There have been experimental and computational efforts investigating the performance of miniature nozzles.[8,9] Established approaches to optimization of nozzles breakdown at lower Reynolds numbers, where viscous effects begin to become more prevalent. [10,11] At the miniature scale, the predominance of viscous effects is amplified.[3] Furthermore, the nature of the MEMS manufacturing process results in rectangular rather than circular nozzles. Depending on the aspect ratio of the nozzle, the top and bottom wall boundaries are likely to heavily influence the flowfield behavior. These physical differences of nozzles at the miniature scale indicate a different optimization of performance.

Challenge	**Issue**
Micro-Thruster Fabrication	Large depths (>200 μm) needed with tight tolerances on throat dimensions and low-temperature bonding
Micro-Nozzle Optimization	Viscous-dominated flow in rectangular nozzle
Propellant Selection	Need high-performance, low-heat flux, benign propellant that is compatible with laser initiation
Diode Laser Initiation	Need to establish parameters for low-power, reliable initiation
Array System Integration	Need efficient packaging of microthrusters, switching of fiber optics, and sequencing of thruster firing

Table I: Technical Challenges for Decomposing Solid Micropropulsion Concept

This report summarizes the performance testing of miniature, rectangular nozzles on ambient-temperature nitrogen and helium gases. The nitrogen test data has been previously reported,[12] although there was an error in reporting the flowrate data that will be corrected in this report. The helium test data is being reported for the first time here. Modeling of these micronozzle contours has been conducted using ambient-temperature nitrogen[13] and simulated combustion products of a decomposing solid propellant.[14] The modeling and experimental are complimentary efforts aimed at determining the optimal area ratio and configuration of micronozzles over a range of gas flow conditions (molecular weight, temperature).

Test Apparatus and Procedure

Thruster/Holder Assembly

All testing was conducted using miniature thruster half-sections fabricated from 500-µm thick silicon wafers. The basic thruster half-section contour is as shown in Figure 1. This contour is a laboratory design and doesn't represent an engineering model configuration. The designed chamber diameter was 6.35 mm. The chamber-to-throat contraction angle was 49.5˚. The design throat widths was 350-µm, while the throat depth and length was 300 µm. The nozzle expansion angle was 27.7˚ and the nominal area ratios were 1, 5, 10, 15, 18.25, 20, and 25. When the thruster half-sections were actually fabricated, there was considerable variability in the dimensions.

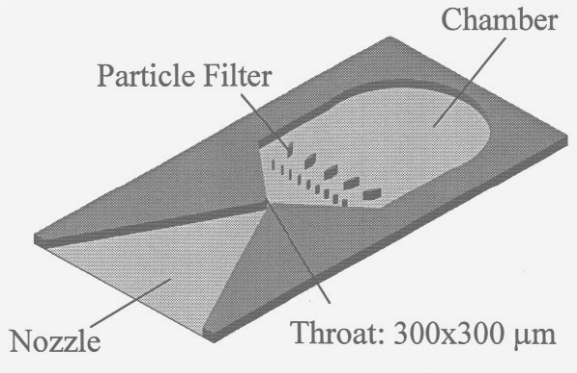

Figure 1: Micronozzle thruster contour

The miniature thruster half-sections were installed in custom made thruster holders (Figure 2), which were then mounted to the thrust stand. The assembly had a small line for the gas inlet, with ports for pressure and temperature measurements. A method was developed to seal the thruster half section within the stainless steal thruster holder. With two hard surfaces, the smallest flaws on either piece could cause a fracture in the brittle silicon wafer. A thin-film gel was used to seal the thruster to its holder, with moderate clamping action applied to obtain a good seal without cracking the brittle thruster. Under pressure, the gel will deform to the imprint of the thruster, and slightly decrease the flowpath cross section. The soft interface is also intended to distribute the loading on the wafer more evenly. A matching backing is applied on the back surface of the half thruster. However, at the parts where there is virtually no loading, i.e. the etched surface of the thruster, bowing will occur, stressing the silicon wafer. On a couple of occasions, the thruster cracked precisely down the center of the inner chamber, clearly due to this loading stress. For each thruster/holder assembly, leak tests were performed by pressurizing the feed system and thruster assembly to a pressure of 0.7 MPa. Only leak-free assemblies continued to be tested.

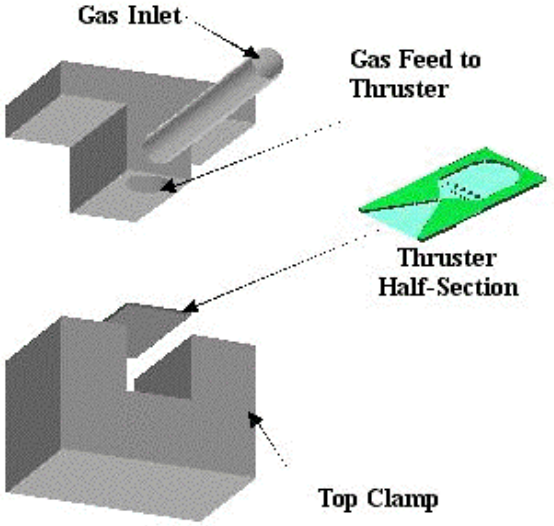

Figure 2: Schematic of thruster holder

Test Facility/Setup

Experiments were performed inside one of NASA GRC's vacuum facilities, a 200-cubic foot test tank, equipped with a 2-foot and a 3-foot diameter port, both isolated from the main test tank through hydraulic valves. This allows interchange of test hardware without the need to fully recycle the tank vacuum. Dual diffusion pumps are able to maintain a vacuum down to 8×10^{-7} torr with low flow rate. At increasing flow rate, tank pressure will rise, up to approximately 7.5×10^{-4} torr with 15000 sccm of nitrogen, at which point the diffusion pumps are set to shut off, and mechanical pumps will take over. Two ion gages at either side of the tank monitor tank pressure.

A schematic of the test setup is shown in Figure 3. Chamber pressure was measured in the feed system slightly upstream of the chamber with a 200 psi, high-frequency, piezoelectric pressure transducer. Temperature was monitored with a type-K thermocouple. A Labview digital data acquisition system was used to record thrust, pressure and temperature, at a 50-Hz data rate. A strip chart recorder was also used to provide real time thrust measurement. Vacuum tank pressure and barometric pressure were manually recorded from facility monitors. A bank of five flow controllers of varying ranges (10, 100, 1000, 10000, and 22000 sccm nitrogen), mounted in parallel, were used to set the volumetric flowrate.

An inverted pendulum thrust stand was used for testing with nitrogen. The thrust stand had been used

previously in the testing of electric propulsion thrusters, such as arcjets, Hall thrusters, and MPD thrusters.[15] Figure 4 show the thruster assembly mounted on a bracket, which in turn is mounted on the thrust stand. Thrust stand capability ranged from less than a milliNewton to over a Newton. A torsional-type thrust stand was used in the helium test series. This is a more sensitive thrust stand used in the testing of pulsed plasma thrusters (PPT's).[16] In both thrust stands, thrust was determined by the deflection of the stand as measured by a LVDT. In all testing, thrust calibrations were conducted directly before each test.

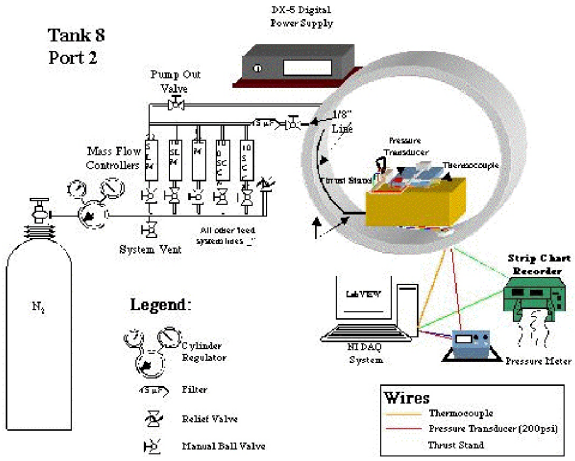

Figure 3: Schematic of Test Setup

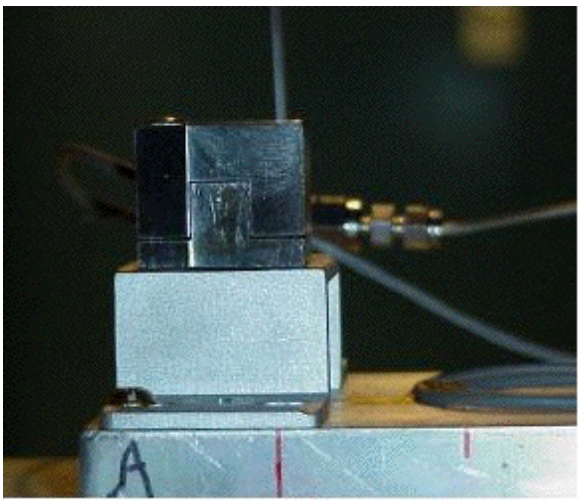
Figure 4: Thruster Assembly Mounted on Thrust Stand, View of Nozzle Exit (Not Discernable in Holder)

Test Procedure/Data Reduction

For all testing, the desired flowrate was set by the mass flow controllers. Test runs were typically 160 seconds in duration, sufficiently long to perform a calibration on the thrust stand, start the gas flow, and allow the thrust and pressure to reach steady state. A steady-state thrust signal was usually achieved within 5 seconds from the start of the gas flow. Digital data were recorded in 0.02-second intervals. In the thrust calibration, three weights (whose mass was measured precisely) stringed on a filament wire were successively applied to the thrust stand and then removed.

In the spreadsheet data file, an average of 100 points on each "step" (including the zeroes) was used to represent a data point on the calibration curve. A least squares fit was done of the calibration data (both the upward and downward curves). The curve fit parameters were used to determine thrust from the steady-state portion of the curve. An average of 1000 points, taken well into the steady-state region, was used to represent the thrust reading. Some fluctuations in the thrust level existed, but it was less then 3% of the nominal thrust level. The measured thrust was corrected to vacuum thrust by adding the product of the vacuum pressure and the nozzle exit area.

Gage chamber pressure was corrected to absolute pressure using a barometric pressure reading taken in the facility. An average of 1000 points in the steady-state region were used (simultaneous with the thrust measurement) to represent the chamber pressure reading.

In the nitrogen series, testing was conducted at flowrates of 10, 20, 50, 100, 200, 500, 1000, and 2900 sccm of nitrogen. For higher area ratio thrusters, testing was also done at 4350, 5800, 7250, and 8700 sccm of nitrogen. Testing was started at 10 sccm, increased to the maximum allowable by the capacity of the diffusion pumps, then decreased back to 10 sccm. In this way, two sets of measurements were obtained at each flow rate (except for the maximum). A similar procedure was used in the helium testing, with the volumetric flowrates set the same as in the nitrogen testing, but with the mass flowrate corrected for helium.

Bias Error in Test Data

Thrust coefficient performance data for nozzles tested with ambient-temperature nitrogen were previously reported in Reference 12. The modeling effort on these nozzles at Penn State lead to a determination that the measured flow rates and chamber pressures were in disagreement. In most cases, characteristic velocity and specific impulse values based on pressure and thrust measurements were much higher than maximum theoretical for the mass flowrate measurements. This indicated a

significant error in one or more of the measured parameters. The calculation of thrust coefficient (from the measured thrust, chamber pressure, and throat area) as the nozzle performance parameter did not reveal this discrepancy.

The experimental setup was disassembled before the discrepancy was discovered, however, an examination of the test procedures for determining each of the measured parameters suggests the source of the error. The measured parameters were,

- Throat Area, determined from measurements of the throat width and depth, using either a scanning electron microscope (SEM) or a measuring microscope

- Chamber Temperature, measured at the inlet tube of the holder (just upstream of the micronozzle chamber), using a chromel-alumel thermocouple

- Chamber Pressure, measured at the inlet tube of the holder (just upstream of the micronozzle chamber), using a 0 to 200 psig dynamic pressure transducer and corrected to psia, using a barometric pressure gauge in the vacuum test facility

- Mass Flowrate, determined from the volumetric flowrate set by a bank of five volumteric flow controllers (10, 100, 1000, 10000, and 22000 sccm nitrogen), corrected to mass flowrate according to the gas used

- Vacuum Thrust, determined from the site thrust measured directly on the thrust stand and corrected to vacuum thrust. The product of the tank pressure (assumed to be the nozzle exit pressure) measured from two ion gauges in the tank and the nozzle exit area, determined from measurements of the nozzle width and throat depth (assumed to be the same as the exit depth) using an measuring microscope, is added to the measured thrust

The source of error cannot be determined definitely, since the experimental setup had been long since disassembled when the error was discovered. All of the flow controllers were calibrated before testing. A small leak in the large flow controllers feeding the same manifold as the smaller flow controllers could have lead to erroneously low mass flowrate measurements at the small flowrates used in the testing. Each flow controller was isolated with a hand valve, which had to leak as well. The pressure transducer was also calibrated before testing and there was no indication of improper operation during testing. An error in the thermocouple used for stagnation temperature would have been obvious during testing as an open circuit. The dimensional measurements (throat and nozzle exit) were made in a procedure described in Reference 12. The errors in those measurements are given in Table II (the measurements made with SEM are noted in the table). They are not large enough to account for the large errors indicated in the performance parameters.

The rocket performance parameters that can be calculated from the basic measurements are,

- Characteristic Velocity (C*) =
  Chamber Pressure * Throat Area/ Mass Flowrate

- Thrust Coefficient (Cf) =
  Vacuum Force/(Chamber Pressure* Throat Area)

- Specific Impulse (Isp) =
  Vacuum Force/Mass Flowrate

Generically, C* measures chamber performance (upstream of the throat), Cf measures nozzle performance (downstream of the throat), and Isp is an overall measure of rocket performance. C* and Isp were higher than theoretically possible, in most cases, significantly higher. The error increased as the flowrate decreased and was substantial for flowrates below 100 sccm. Cf, however, was very low, which seemed to be reasonable for miniature, rectangular nozzles, dominated by viscous flows.

The evidence, then, points to an error in the mass flowrate, since they are in denominator of both equations for C* and Isp, while it is absent from the Cf equation. If the actual mass flowrate was much higher than the flowrate thought to be set by the flow controllers, then both C* and Isp would be inflated, while Cf would be unaffected. If an inflated vacuum force was responsible for the high Isp values, then it would not be reflected in the C* numbers. In the same line of reasoning, if an inflated chamber pressure was responsible for the high C* numbers, then Isp would not be affected. Of course, there is the possibility that both vacuum force and chamber pressure were inflated, canceling each other in the Cf equation. There is no definite way of disproving this assertion, although, two different thrust stands were used for the nitrogen and helium testing. Since the error occurred in both test series, it seems unlikely that a bias existed in both thrust stands.

Nozzle ID (Series)	Area Ratio	Throat Width (µm) Error (%)	Exit Width (µm) Error (%)	Depth (µm) Error (%)
146 (N2)	1.0	372 0.2%	372 0.2 %	295 5.8 %
153 (N2 & He)	1.5	230 (SEM) 8.9 %	353 (SEM) 5.8 %	271 (Est.) 7.0 %
169 (N2)	4.8	367 0.3 %	1756 0.2 %	198 3.4 %
170 (He)	4.8	366 0.2 %	1761 0.2 %	246 4.8 %
178 (N2)	9.7	362 0.3 %	3511 0.04 %	260 1.8 %
182 (He)	9.7	362 0.1 %	3510 0.01 %	385 2.5 %
195 (He)	14.5	362 0.3 %	5260 0.01 %	238 4.0 %
208 (N2)	14.9	353 0.8 %	5246 0.1 %	220 8.6 %
226 (N2 & He)	18.3	380 (SEM) 4.2 %	6933 (SEM) 2.7 %	243 (Est.) 5.8 %
230 (N2)	19.5	360 0.2 %	7008 0.1 %	243 3.2 %
243 (N2 & He)	23.1	367 (SEM) 3.3 %	8467 (SEM) 1.8 %	214 (Est.) 3.1 %
237 (N2)	24.2	361 0.3 %	8759 0.01 %	221 15.7 %

Table II: Dimensional Measurements of Micronozzles

All of the testing was conducted using a bank of mass flow controllers, ranging from 10 to 22,000 sccm, arranged in parallel. When the test apparatus was put together, it was thought that testing would be conducted well above 10,000 sccm. Testing always started at 10 sccm and most of the data was gathered at points below 2900 sccm (usually above that value, the vacuum in the test tank was compromised). Any small addition of gas flow to the system could seriously bias the volumetric flowrate values. This rationale seems to be supported by the fact that the larger errors occurred at the small flowrate values. Figures 5 and 6 plot the C* values versus volumetric flowrate for nitrogen and helium, respectively. There clearly is an error in most, if not all, of the values, but the error increases greatly as flowrate decreases.

The above arguments seem to suggest an undetected bias in the volumetric flowrate measurements in both test series. The bias had the affect of creating a larger flowrate than indicated by the instrumentation. If there is error in the flowrate measurements, then the Reynolds number calculations are in error (lower than the actual value). The same is true of the performance parameters calculated using mass flowrate (C* and Isp), as well as theoretical thrust calculated from isentropic relations. However, there is no reason to suspect the force measurements, particularly since two different thrust stands were used in the nitrogen and helium testing. Thus, the data collected can be accurately presented in terms of thrust coefficient versus stagnation pressure for a given set of area ratios, but the calculated Reynolds number is low by orders of magnitude at the lowest flowrates.

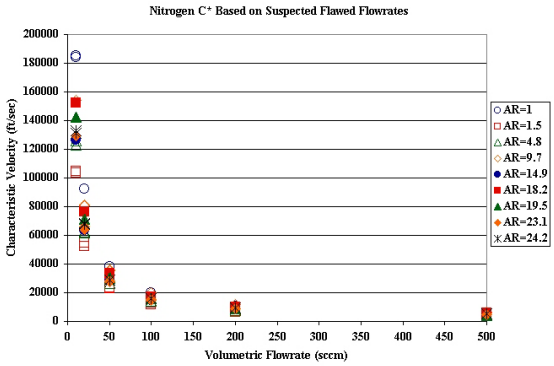

Figure 5: Nitrogen C* Performance Based on Suspected Bias Flowrate Data

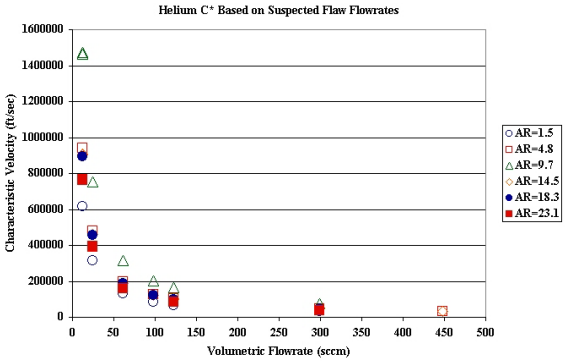

Figure 6: Helium C* Performance Based on Suspected Bias Flowrate Data

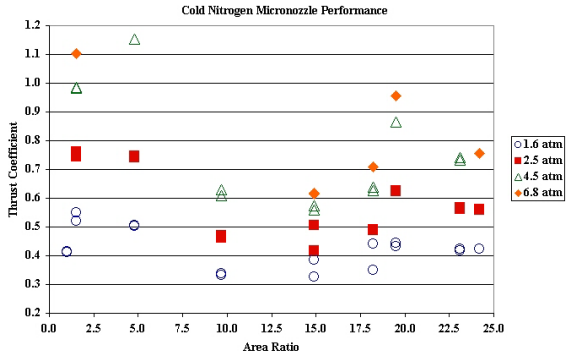

Figure 7: Thrust Coefficient vs. Area Ratio for Cold Gas Nitrogen

Test Data

Despite the issues with the flowrate data, the conclusions drawn in the previous report did not change. Figure 7 plots the thrust coefficient versus area ratio for four sets of chamber pressures. In Figure 8, thrust coefficient is plotted against chamber pressure for each nozzle (set of area ratios). Appendix A lists the same data in tabular format. The data shows that nozzle performance increases to a maximum around area ratio 5, then drops off sharply to a minimum between area ratio 10 and 15. Above area ratio 15, however, there is another performance increase until a secondary maximum around area ratio 20. The data are consistent with computational results using Direct Simulation Monte Carlo (DSMC) in a three-dimensional contour, out to area ratio 10, which show a maximum thrust at an area ratio of 6.[13]

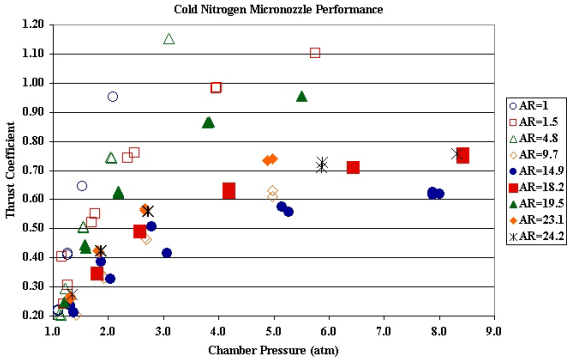

Figure 8: Thrust Coefficient vs. Chamber Pressure for Cold Gas Nitrogen

Figure 9 plots thrust coefficient versus area ratio over three sets of chamber pressures for the thrusters tested with cold helium gas. Figure 10 shows thrust coefficient versus chamber pressure for each nozzle (set of area ratios). Appendix B lists the same data in tabular format. There are fewer data points than the nitrogen test series, but the maximum performance was achieved at the lowest area ratio tested (1.5). Performance decreased after this point, with a minimum occurring around area ratio 10. As with the nitrogen test series there was an increase in performance above area ratio 15. Unlike the nitrogen flow, this performance increase continued beyond area ratio 20, although there were few data points to draw conclusions from.

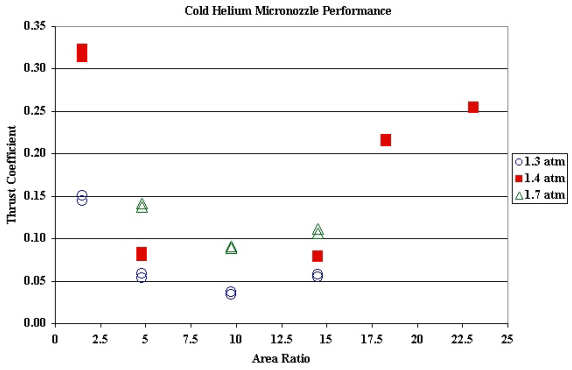

Figure 9: Thrust Coefficient vs. Area Ratio for Cold Gas Helium

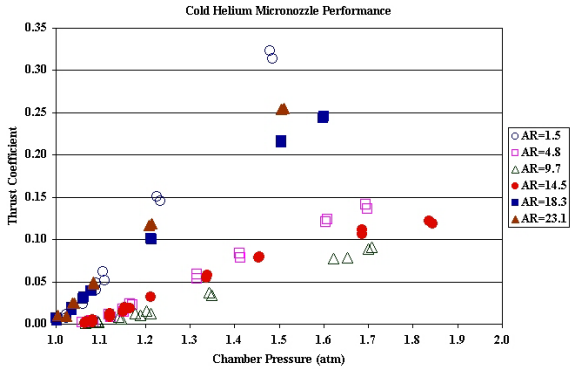

Figure 10: Thrust Coefficient vs. Chamber Pressure for Cold Gas Helium

Figures 11, 12, and 13 compare nitrogen and helium thrust coefficients for nozzles with area ratio nozzles 1.5, 18.3, and 23.1, respectively. The nitrogen flows always provide better nozzle performance than helium at chamber pressures below 1.6 atm. However, the slope of the helium curve was steeper than the nitrogen curve, suggesting that at higher chamber pressures, helium flows would provide better performance than nitrogen.

Thrusters in a decomposing solid micropropulsion system could be sized for a range of chamber pressures, even within the same array, depending on the propulsion function desired. The propellants used in the concept are likely to produce primarily nitrogen,[7] so there may be a performance advantage to operating at 1 to 2 atm chamber pressure.

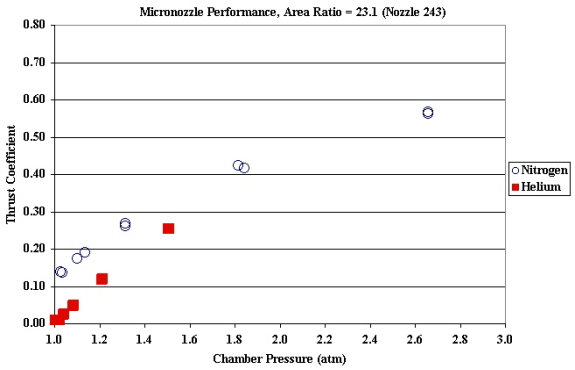

Figure 11: Nitrogen and Helium Nozzle Performance for Area Ratio = 1.5 (Micronozzle 153)

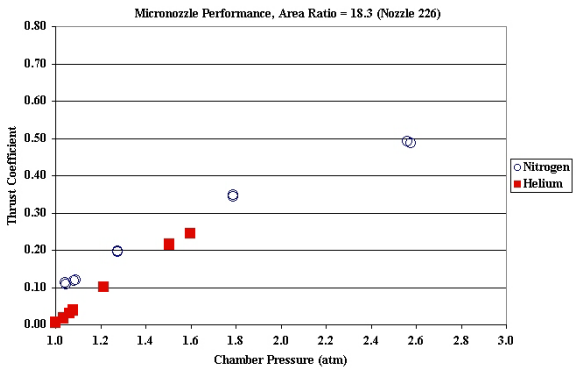

Figure 12: Nitrogen and Helium Nozzle Performance for Area Ratio = 18.3 (Micronozzle 226)

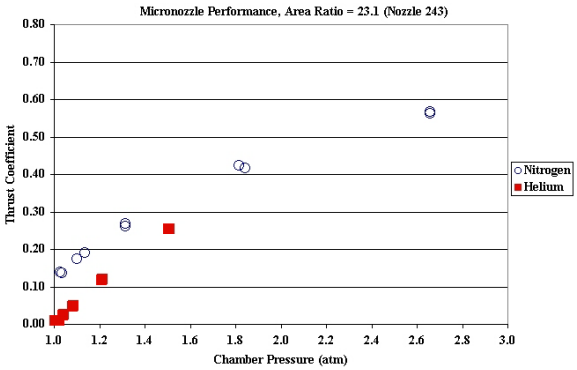

Figure 13: Nitrogen and Helium Nozzle Performance for Area Ratio = 23.1 (Micronozzle 243)

Summary

A micropropulsion concept that utilizes decomposing solid propellants offers many advantages for small and miniature spacecraft. However, there are many technical challenges facing the development of this concept, including performance of the rectangular micronozzles. Testing has been conducted of flat micronozzles under ambient-temperature nitrogen and helium flows. This testing, in conjunction with numerical modeling, has indicated that a short area ratio will provide the best performance for micronozzles. Testing with nitrogen showed a performance peak around area ratio 5, which is consistent with computational modeling that has been conducted. Testing with helium flows showed performance peaking at area ratio 1.5, suggesting that no nozzles might be best for these flows. Testing with nitrogen and helium flows both indicated performance minimums around area ratio 10 and secondary performance peaks above area ratio 15. Testing with ambient-temperature flows in flat, rectangular micronozzles are the first step to understanding nozzle optimization at this scale. More testing needs to be conducted to understand the influence of throat area (small throat widths), throat aspect ratio (larger depths), and gas temperature

(heated flows) on the performance of these non-optimized nozzles.

References

1. Collins, D., Kukkonen, C., and Venneri, S., "Miniature, Low-Cost, Highly Autonomous Spacecraft – A Focus for the New Millennium," IAF 95-U.2.06, 46th International Astronautical Congress, Oslo, Norway, October 1995.
2. Proceedings of the AFOSR/DARPA/AFRL/VSD Micro/Nanotechnology for Micro/Nanosatellites workshop, Edited by A. Das, Alburqueque, NM, April 1998.
3. Ketsdever, A. and Mueller, J., "Systems Considerations and Design Options for Microspacecraft Propulsion Systems," AIAA 99-2723, 35th Joint Propulsion Conference, Los Angeles, CA, June 1999.
4. Janson, S., "Chemical and Electric Micropropulsion Concepts for Nanosatellites," AIAA Paper 94-2998, 30th Joint Propulsion Conference, Indianapolis, IN, July 1994.
5. de Groot W. and Oleson, S., "Chemical Microthruster Options," AIAA Paper 96-2868, 32nd Joint Propulsion Conference, Lake Buena Vista, FL, July 1996.
6. Mueller, J., "Thruster Options for Microspacecraft: A Review and Evaluation of Existing Hardware and Emerging Technologies," AIAA Paper 97-3058, 33nd Joint Propulsion Conference, Seattle, WA, July 1997.
7. de Groot, W., Reed, B., and Brenizer, M., "Preliminary Results of Solid Gas Generator Micropropulsion," NASA TM-1999-208842, AIAA 98-3225, 34nd Joint Propulsion Conference, Cleveland, OH, July 1998.
8. Bayt, R., Ayon, A., and Breuer, K., "A Performance Evaluation of MEMS-based Micronozzles," AIAA 97-3169, 33nd Joint Propulsion Conference, Seattle, WA, July 1997.
9. Alexeenko, A., Levin, D., Gimelshein, S., Collins, R., and Markelov, G., "Numerical Simulation of High-Temperature Gas Flows in a Millimeter-Scale Thruster," AIAA 2001-1011, 39th Aerospace Sciences Meeting, Reno, NV, January 2001.
10. Grisnik, S., Smith, T., and Saltz, L., "Experimental Study of Low Reynolds Number Nozzles," AIAA Paper 87-0992, 19th International Electric Propulsion Conference, Colorado Springs, CO, 1987.
11. Arrington, L., Reed, B., and Rivera, A., "A Performance Comparison of Two Small Rocket Nozzles," AIAA 96-2582, 32nd Joint Propulsion Conference, Lake Buena Vista, FL, July 1996.
12. Reed, B., de Groot, W., and Dang, L., "Experimental Evaluation of Cold Flow Micronozzles," AIAA 2001-3521, 37th Joint Propulsion Conference, Salt Lake City, UT, July 2001.
13. Alexeenko, A., Levin, D., Gimelshein, S., Collins, R., and Reed, B., "Numerical Modeling of Axisymmetric and Three-Dimensional Flows in Microelectromechanical Systems Nozzles," AIAA Journal, Vol. 40, No. 5, pp. 897-904.
14. Alexeenko, A., Levin, D., Gimelshein, S., Collins, R., and Reed, B., "Numerical Study of Flowfield Structure and Thrust Performance for 3-D MEMS-Based Nozzles," 32nd AIAA Fluid Dynamics Conferences, St. Louis, MO, June 2002.
15. Haag, T., "Thrust Stand for High-Power Electric Propulsion Devices," Rev. Sci. Instrum., Vol. 62, No. 5, pp. 1186-1191, May 1991.
16. Haag, T., "Thrust Stand for Pulsed Plasma Thrusters," Rev. Sci. Instrum., Vol. 68, No. 5, pp. 2060-2067, May 1997.

Appendix A: Cold Gas Nitrogen Micronozzle Performance Data

Nozzle 146, Area Ratio = 1.0

Chamber Pressure (atm)	Vacuum Thrust (mN)	Thrust Coefficient
1.00	0.722	0.067
1.00	0.713	0.066
1.00	0.761	0.070
1.00	0.893	0.083
1.03	0.649	0.058
1.03	1.16	0.103
1.07	1.72	0.149
1.07	1.66	0.143
1.12	2.65	0.219
1.12	2.68	0.222
1.29	5.77	0.415
1.29	5.75	0.411
1.56	10.9	0.644
1.57	10.9	0.645
2.13	22.0	0.954

Nozzle 153, Area Ratio = 1.5

Chamber Pressure (atm)	Vacuum Thrust (mN)	Thrust Coefficient
1.00	0.771	0.127
1.00	0.837	0.137
1.03	0.924	0.145
1.00	0.860	0.141
1.11	1.19	0.174
1.09	1.06	0.158
1.22	1.82	0.243
1.12	1.36	0.198
1.18	2.93	0.403
1.29	2.42	0.306
1.80	6.10	0.392
1.73	5.56	0.522
2.53	11.8	0.761
2.40	10.9	0.743
4.03	24.3	0.983
4.05	24.5	0.985
5.87	39.8	1.10

Nozzle 169, Area Ratio = 4.8

Chamber Pressure (atm)	Vacuum Thrust (mN)	Thrust Coefficient
1.01	0.720	0.098
1.00	0.821	0.114
1.00	0.800	0.110
1.00	0.792	0.109
1.05	1.12	0.147
1.05	1.18	0.154
1.14	1.70	0.204
1.11	1.68	0.207
1.22	2.61	0.293
1.21	2.61	0.295
1.54	5.66	0.503
1.55	5.71	0.506
2.06	11.2	0.742
2.03	11.1	0.746
3.10	26.0	1.15

Nozzle 178, Area Ratio = 9.7

Chamber Pressure (atm)	Vacuum Thrust (mN)	Thrust Coefficient
1.00	0.880	0.098
1.00	0.785	0.087
1.00	0.829	0.088
1.00	0.937	0.100
1.10	1.07	0.103
1.10	1.14	0.109
1.23	1.58	0.136
1.24	1.66	0.141
1.43	2.68	0.198
1.42	2.72	0.203
1.92	6.00	0.331
1.90	6.08	0.337
2.70	11.8	0.463
2.66	11.9	0.470
4.97	28.7	0.609
4.98	29.7	0.630

Nozzle 208, Area Ratio = 14.9

Chamber Pressure (atm)	Vacuum Thrust (mN)	Thrust Coefficient
1.00	0.850	0.115
1.00	0.785	0.106
1.00	0.836	0.111
1.06	1.15	0.139
1.05	0.996	0.121
1.11	1.33	0.153
1.11	1.33	0.153
1.31	2.41	0.236
1.37	2.26	0.211
1.86	5.60	0.385
2.03	5.19	0.326
2.78	11.0	0.506
3.06	9.98	0.417
5.15	23.2	0.575
5.27	23.0	0.558
7.88	38.0	0.616
8.01	38.7	0.618
7.88	38.5	0.625

Nozzle 226, Area Ratio = 18.2

Chamber Pressure (atm)	Vacuum Thrust (mN)	Thrust Coefficient
1.00	0.910	0.102
1.00	0.879	0.099
1.00	0.806	0.090
1.00	0.811	0.091
1.04	1.09	0.113
1.05	1.06	0.109
1.09	1.21	0.119
1.08	1.19	0.119
1.27	2.35	0.198
1.27	2.32	0.196
1.79	5.80	0.242
1.79	5.72	0.344
2.58	11.7	0.488
2.56	11.7	0.492
4.19	24.8	0.637
4.18	24.3	0.626
6.43	42.4	0.709
8.43	58.4	0.745
8.42	59.4	0.758
10.2	74.2	0.780
10.2	74.1	0.780
12.4	97.3	0.842

Nozzle 230, Area Ratio = 19.5

Chamber Pressure (atm)	Vacuum Thrust (mN)	Thrust Coefficient
1.00	0.843	0.101
1.00	0.770	0.093
1.00	0.838	0.101
1.00	0.881	0.106
1.00	1.23	0.139
1.01	1.14	0.128
1.06	1.58	0.169
1.06	1.51	0.161
1.20	2.62	0.248
1.20	2.61	0.247
1.59	6.06	0.433
1.58	6.20	0.445
2.18	11.9	0.623
2.18	12.0	0.626
3.82	29.2	0.866
3.79	28.9	0.864
5.50	46.3	0.955

Nozzle 243, Area Ratio = 23.1

Chamber Pressure (atm)	Vacuum Thrust (mN)	Thrust Coefficient
0.96	0.854	0.113
0.96	0.822	0.109
0.95	0.872	0.116
0.97	0.861	0.112
1.03	1.12	0.138
1.03	1.12	0.138
1.10	1.51	0.173
1.14	1.71	0.191
1.32	2.79	0.269
1.32	2.71	0.260
1.84	6.07	0.417
1.82	6.07	0.423
2.66	11.8	0.562
2.66	12.0	0.568
4.88	28.3	0.733
4.97	29.1	0.740
9.33	62.3	0.845
9.31	62.0	0.844
12.8	88.4	0.877

Nozzle 237, Area Ratio = 24.2

Chamber Pressure (atm)	Vacuum Thrust (mN)	Thrust Coefficient
0.97	0.911	0.117
0.95	0.789	0.103
0.98	0.900	0.114
0.99	0.907	0.114
1.04	1.26	0.151
1.04	1.08	0.129
1.16	1.81	0.194
1.16	1.85	0.198
1.34	2.96	0.275
1.34	2.94	0.274
1.86	6.37	0.425
1.86	6.35	0.425
2.72	12.2	0.559
2.71	12.2	0.561
5.87	33.6	0.710
5.88	34.5	0.729
8.32	50.7	0.757

Appendix B: Cold Gas Helium Micronozzle Performance Data

Nozzle 153, Area Ratio = 1.5

Chamber Pressure (atm)	Vacuum Thrust (mN)	Thrust Coefficient
1.00	0.028	0.005
1.00	0.023	0.004
1.02	0.049	0.008
1.02	0.070	0.011
1.06	0.159	0.024
1.06	0.200	0.030
1.09	0.278	0.041
1.09	0.334	0.049
1.11	0.360	0.052
1.11	0.429	0.062
1.23	1.12	0.145
1.23	1.16	0.151
1.49	2.93	0.314
1.48	3.00	0.323

Nozzle 170, Area Ratio = 4.8

Chamber Pressure (atm)	Vacuum Thrust (mN)	Thrust Coefficient
1.06	0.019	0.002
1.08	0.023	0.002
1.08	0.043	0.004
1.12	0.086	0.008
1.12	0.115	0.011
1.15	0.148	0.014
1.15	0.188	0.018
1.17	0.247	0.023
1.17	0.240	0.023
1.32	0.640	0.054
1.31	0.702	0.059
1.41	1.01	0.079
1.41	1.07	0.084
1.61	1.76	0.121
1.61	1.81	0.124
1.70	2.10	0.137
1.69	2.17	0.141

Nozzle 182, Area Ratio = 9.7

Chamber Pressure (atm)	Vacuum Thrust (mN)	Thrust Coefficient
1.07	0.015	0.001
1.07	0.027	0.002
1.10	0.032	0.002
1.09	0.052	0.003
1.15	0.102	0.006
1.14	0.131	0.008
1.19	0.172	0.010
1.18	0.208	0.013
1.21	0.216	0.013
1.20	0.261	0.015
1.35	0.645	0.034
1.34	0.697	0.037
1.62	1.75	0.077
1.65	1.83	0.079
1.70	2.12	0.089
1.71	2.18	0.091

Nozzle 195, Area Ratio = 14.5

Chamber Pressure (atm)	Vacuum Thrust (mN)	Thrust Coefficient
1.06	0.007	0.001
1.07	0.026	0.003
1.08	0.019	0.002
1.08	0.049	0.005
1.12	0.081	0.008
1.12	0.122	0.013
1.15	0.146	0.015
1.15	0.194	0.019
1.17	0.186	0.018
1.21	0.337	0.032
1.34	0.633	0.055
1.34	0.674	0.058
1.45	0.982	0.078
1.46	1.00	0.079
1.69	1.55	0.106
1.69	1.63	0.111
1.84	1.89	0.118
1.84	1.93	0.122

Nozzle 226, Area Ratio = 18.2

Chamber Pressure (atm)	Vacuum Thrust (mN)	Thrust Coefficient
1.00	0.034	0.004
1.00	0.000	0.000
1.00	0.069	0.007
1.00	0.040	0.004
1.04	0.190	0.020
1.03	0.162	0.017
1.06	0.314	0.032
1.06	0.296	0.030
1.08	0.395	0.039
1.08	0.389	0.039
1.21	1.13	0.100
1.21	1.15	0.102
1.51	3.01	0.215
1.51	3.03	0.217
1.60	3.63	0.244
1.60	3.65	0.246

Nozzle 243, Area Ratio = 23.1

Chamber Pressure (atm)	Vacuum Thrust (mN)	Thrust Coefficient
1.00	0.041	0.005
1.00	0.033	0.004
1.00	0.082	0.010
1.02	0.074	0.009
1.04	0.205	0.025
1.04	0.200	0.024
1.08	0.421	0.049
1.08	0.408	0.048
1.21	1.11	0.117
1.21	1.14	0.119
1.51	3.04	0.255
1.50	3.02	0.254

REPORT DOCUMENTATION PAGE

Form Approved
OMB No. 0704-0188

1. AGENCY USE ONLY (*Leave blank*)	2. REPORT DATE	3. REPORT TYPE AND DATES COVERED
	May 2003	Technical Memorandum

4. TITLE AND SUBTITLE

Decomposing Solid Micropropulsion Nozzle Performance Issues

5. FUNDING NUMBERS

WBS–22–755–70–00–02

6. AUTHOR(S)

Brian Reed

7. PERFORMING ORGANIZATION NAME(S) AND ADDRESS(ES)

National Aeronautics and Space Administration
John H. Glenn Research Center at Lewis Field
Cleveland, Ohio 44135–3191

8. PERFORMING ORGANIZATION REPORT NUMBER

E–13845

9. SPONSORING/MONITORING AGENCY NAME(S) AND ADDRESS(ES)

National Aeronautics and Space Administration
Washington, DC 20546–0001

10. SPONSORING/MONITORING AGENCY REPORT NUMBER

NASA TM—2003-212225
AIAA–2003–0672

11. SUPPLEMENTARY NOTES

Prepared for the 41st Aerospace Sciences Meeting and Exhibit sponsored by the American Institute of Aeronautics and Astronautics, Reno, Nevada, January 6–9, 2003. Responsible person, Brian Reed, organization code 5430, 216–977–7489.

12a. DISTRIBUTION/AVAILABILITY STATEMENT

Unclassified - Unlimited
Subject Categories: 28 and 20 Distribution: Nonstandard

Available electronically at http://gltrs.grc.nasa.gov

This publication is available from the NASA Center for AeroSpace Information, 301–621–0390.

12b. DISTRIBUTION CODE

13. ABSTRACT ***(Maximum 200 words)***

Micropropulsion technology is essential to the success of miniaturized spacecraft and can provide ultra-precise propulsion for small spacecraft. NASA Glenn Research Center has envisioned a micropropulsion concept that utilizes decomposing solid propellants for a valveless, leak-free propulsion system. Among the technical challenges of this decomposing solid micropropulsion concept is optimization of miniature, rectangular nozzles. A number of flat micronozzles were tested with ambient-temperature nitrogen and helium gas in a vacuum facility. The thrusters were etched out of silicon and had throat widths on the order of 350 microns and throat depths on the order of 250 microns. While these were half-sections of thrusters (two would be bonded together before firing), testing provided the performance trend for nozzles of this scale and geometry. Area ratios from 1 to 25 were tested, with thrust measured using an inverted pendulum thrust stand for nitrogen flows and a torsional thrust stand for helium. In the nitrogen testing, peak nozzle performance was achieved around area ratio of 5. In the helium series, nozzle performance peaked for the smallest nozzle tested area ratio 1.5. For both gases, there was a secondary performance peak above area ratio 15. At low chamber pressures (< 1.6 atm), nitrogen provided higher nozzle performance than helium. The performance curve for helium was steeper, however, and it appeared that helium would provide better performance than nitrogen at higher chamber pressures.

14. SUBJECT TERMS

Micropropulsion; Nozzle; Spacecraft

15. NUMBER OF PAGES

19

16. PRICE CODE

17. SECURITY CLASSIFICATION OF REPORT	18. SECURITY CLASSIFICATION OF THIS PAGE	19. SECURITY CLASSIFICATION OF ABSTRACT	20. LIMITATION OF ABSTRACT
Unclassified	Unclassified	Unclassified	